Developments in the fracture and fatigue assessment of materials and structures

Visual Abstract

Effect of additive elements Bi/Ni/Ge on crack initiation and propagation for low-Ag solders

Noritake Hiyoshi
University of Fukui, Japan
hiyoshin@u-fukui.ac.jp

Mitsuo Yamashita
Tohoku University, Japan
mitsuo-yamashita@jcom.home.ne.jp

Hiroaki Hokazono
Fuji Electric Co., Ltd., Japan
hokazono-hiroaki@fujielectric.com

ABSTRACT. This study discusses an effect of additive elements on crack propagation behaviour for low-Ag contain Sn1.0Ag0.7Cu lead-free solders at high temperature. A cyclic push-pull loading tests for four kinds of Sn1.0Ag0.7Cu solders were conducted at 313 K with a single hole specimen. Stress amplitude of solders containing additive element Bi were bigger than that of Bi-free solders. Crack initiation cycle of solders containing Bi were earlier than that of Bi-free solders. Low-Ag solders containing Bi had shorter crack propagation cycles than that of Bi-free solders. These results indicate that the additive element Bi have the effects on the crack initiation and propagation cycles, that is, Bi accelerates the crack propagation rate. We also discuss the adaptation of J-integral range parameter to the crack propagation rate evaluation for solders. J-integral range parameter evaluates the crack propagation rate for low-Ag solders independent of the additive elements.

KEYWORDS. Additive elements; Crack initiation; Crack propagation; Lead-free solder; Low-Ag.

OPEN ACCESS

INTRODUCTION

Soldering is an important and a fundamental technique for electronic device mounting. It is well known that Sn-Pb solders are not allowed to use because it contains Pb which is a harmful element to the earth environment and human bodies. There are many kinds of candidate lead (Pb)-free solders and it is needed to investigate their

mechanical properties and fatigue life [1]-[6]. Solder joints in electronic devices undergo cyclic fatigue damage caused by not only mechanical loading but also thermal loading due to the mismatch of thermal expansion coefficient of different connecting parts. The solder joints also have lots of stress concentration parts, so that it is useful for fatigue life estimation of electronic devices to make clear the cyclic crack initiation and propagation behaviour of solders from the stress concentration part at commercial operating temperature.

Although Sn-3.0Ag-0.5Cu lead-free solder is widely used solder all over the world, there are some issues for the solder. One of these issues is that high material cost due to it contains Ag element. There are lots of candidate lead-free solders substitute for Sn-3.0Ag-0.5Cu solder in order to reduce the material cost. Sn-low-Ag-Cu solders which is one of the candidate solders have a lower material cost than that of Sn-3.0Ag-0.5Cu solder as reducing Ag element, so that the Sn-low-Ag-Cu solders are useful material for industrial use. The melting point temperature of Sn-low-Ag-Cu solders is 500 K and the material cost is about 4,800JPY (Japanese Yen) per 1kg while Sn-3.0Ag-0.5Cu solder costs about 7,500JPY. Although it is important for commercial safety products design to clarify not only tensile strength and mechanical properties but also fatigue life of the electronic materials, there is little experimental research paper on Sn-low-Ag-Cu solders. There is also little research paper on crack initiation and propagation behaviour of the solders at commercial operating temperatures. The reason for little research paper on the crack investigation of solders might be a difficulty of testing technique for solders which have low strength and small hardness.

This study discusses the crack initiation and propagation behaviour of Sn-low-Ag-Cu solders at high temperature. A cyclic push-pull loading tests with a single hole specimen were conducted to investigate the crack initiation and propagation behaviour of the solders. This study also discusses the adaptation of J-integral range parameter for the crack propagation rate evaluation.

EXPERIMENTAL PROCEDURE

The materials tested in this study are four kinds of low-Ag solders of which chemical composition are listed in Tab. 1. Sn1.0Ag0.7Cu solder (SnAgCu) contains lower Ag element in order to reduce the coarse intermetallic compound forming and to reduce the materials costs. The melting point temperature of SnAgCu is 500 K. Sn1.0Ag0.7CuNiGe solder (SnAgCu+NiGe) is the solder which is added 0.07% Ni and 0.01% Ge to SnAgCu. Sn1.0Ag0.7Cu2.0Bi solder (SnAgCu+Bi) is the solder which is added 2.0% Bi to SnAgCu. Sn1.0Ag0.7Cu2.0BiNiGe solder (SnAgCu+BiNiGe) is the solder which is added 2.0% Bi, 0.07% Ni and 0.01% Ge to SnAgCu.

A cyclic push-pull loading tests were conducted with a single hole specimen. Fig, 1 shows shape and dimensions of the specimen, which has a single through hole with 1mm in diameter at a center of the specimen as a stress concentration part. The specimen has a stress concentration factor of K_t=2.72, which is calculated by using Eqn. (1) [7].

$$K_t = 3.00 - 3.13\left(\frac{d}{W}\right) + 3.66\left(\frac{d}{W}\right)^2 - 1.53\left(\frac{d}{W}\right)^3 \qquad (1)$$

where, d and W is diameter of the center thorough hole and specimen width, respectively. The specimen is produced by a mechanical procedure from a low-Ag solders ingot which were casted under controlled temperature and controlled instruction.
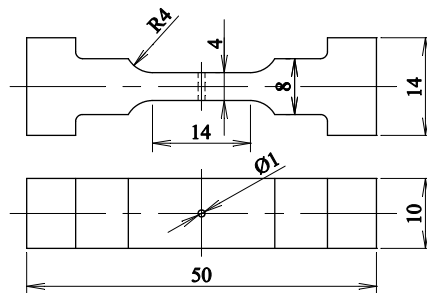

Figure 1: Shape and dimensions of the specimen (mm).

Fig, 2 is a photograph of an electric hydraulic cyclic push-pull loading apparatus for solders. A 10kN small capacity actuator and a 10kN capacity load cell are adapted in order to conduct the fatigue test for solders. The cyclic push-pull

loading tests were conducted under strain control mode with fully reversed symmetrical triangle waveform. The applied strain ratio was $R=-1$. The rapid strain rate of 0.1%/s was used in order to eliminate a creep damage during the cyclic loading. An axial extensometer with linear variable differential transformer was used to measure the axial total strains of 10mm gage part. To avoid unexpected bending deformation of the specimen or unexpected cracking at the location of the extensometer rod tips, two small bumps of epoxy resin with grooves were formed on the specimen surface and the tips of the extensometer rods were placed on the grooves [8].

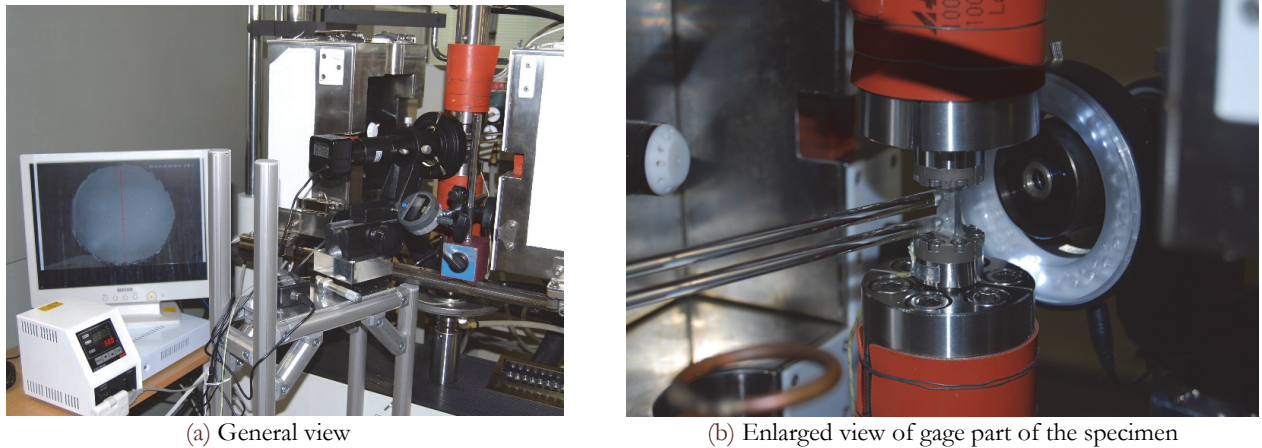| (a) General view | (b) Enlarged view of gage part of the specimen |

Figure 2: Cyclic push-pull loading apparatus with crack observation system.

The specimen was heated up to 313 K with rubber heaters which are attached to both upper and lower connecting rods. We had confirmed in advance that temperature distribution and variation of the specimen during the tests were satisfied with the testing standard for solders [8].

Crack initiation and propagation behaviour was observed with a CCD camera and a LCD monitor. Crack length ($2a$), which is defined as the length from one end to another end of the crack in a horizontal direction including the center through hole, was also measured with the CCD camera view. Crack initiation cycle (N_i) was defined as the cycle of a newly 0.01mm in crack length were observed at the center through hole. The number of cycles to failure (N_f) was defined as the cycle of 25 percent tensile stress amplitude drop from that at a midlife of N_f.

Low-Ag Solders	Sn	Ag	Cu	Bi	Ni	Ge
Sn1.0Ag0.7Cu	Bal.	1.0	0.7	---	---	---
Sn1.0Ag0.7CuNiGe	Bal.	1.0	0.7	---	0.07	0.01
Sn1.0Ag0.7Cu2.0Bi	Bal.	1.0	0.7	2.0	---	---
Sn1.0Ag0.7Cu2.0BiNiGe	Bal.	1.0	0.7	2.0	0.07	0.01

Table 1: Chemical composition of material tested (mass%).

EXPERIMENTAL RESULTS AND DISCUSSION

Stress-strain relationship and crack propagation direction

Fig. 3 shows stress-strain relationship for four kinds of low-Ag solders at 100th cycle. There is stress amplitude difference between SnAgCu / SnAgCu+NiGe Bi-free solders and SnAgCu+Bi / SnAgCu+BiNiGe solders containing Bi. Bigger stress amplitude of SnAgCu+Bi / SnAgCu+BiNiGe solders indicates that Bi element increase the stress amplitude for cyclic loading.

Fig, 4 is a photograph of surface crack observation results after the tests. Main crack initiated from edge of the center through hole and propagated in the maximum shear direction for SnAgCu (photo (a) and (b)). Crack propagation direction of SnAgCu+NiGe were also the maximum shear direction (photo (c) and (d)). On the other hand, crack

propagation direction of solders containing Bi were complicated. One side crack propagated in the principal direction and a propagation direction of another crack changed from the maximum shear direction to the principal direction for SnAgCu+Bi (photo (e) and (f)). Crack propagated in the maximum shear direction for SnAgCu+BiNiGe in the smaller strain range (photo (g)), but crack propagation direction of one side for SnAgCu+BiNiGe in the larger strain range was changed from the principal direction to the maximum shear direction (photo (h)). The crack propagation direction difference and the direction changing behaviour among the low-Ag solders might depend on the existence of Bi element. The detailed crack propagation mechanism and effect of Bi element on the crack propagation direction are still unknown, we need more sufficient crack observations and data analysis.
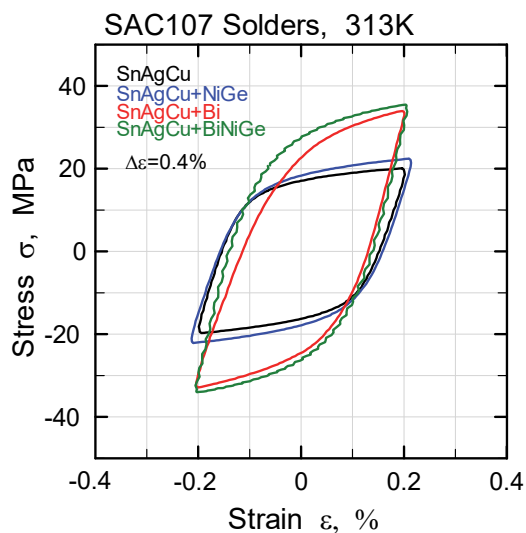

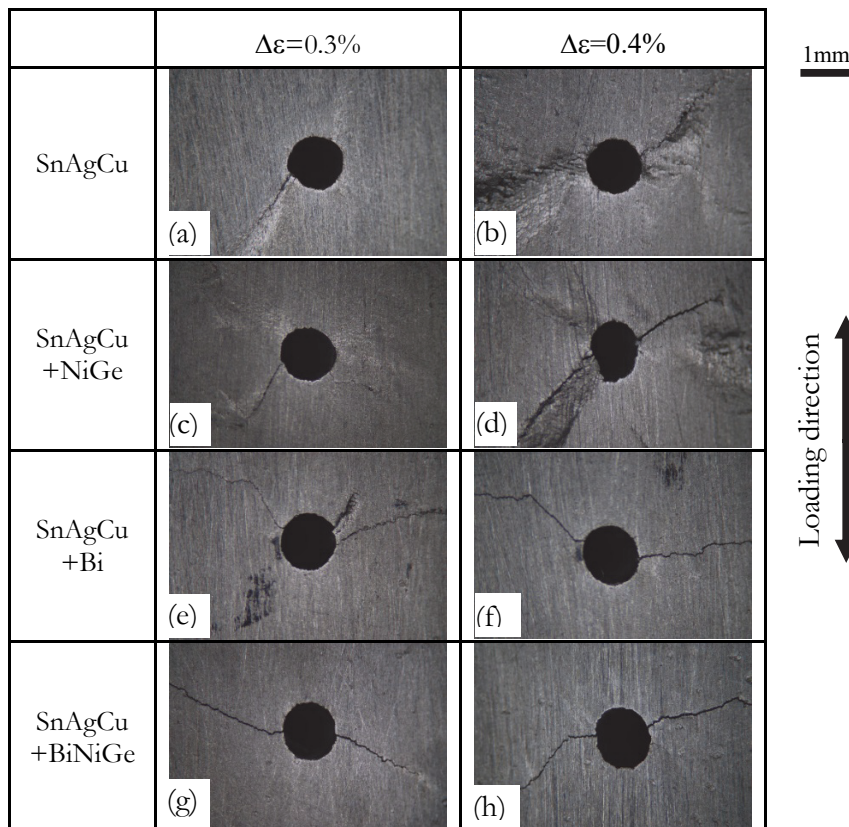Figure 3: Hysteresis loop at 100th cycle.

Figure 4: Crack propagation observations after the tests.

Crack initiation and propagation behaviour

Crack initiation cycle (N_i) are summarized in Tab. 2. Crack initiation cycle ratio (N_i/N_{i-SAC}) which is calculated as division by crack initiation cycle of SnAgCu at same strain range are shown in Fig. 5. Although crack initiation cycle of Bi-free solders were over 1900 cycles, crack initiation cycle of solders containing Bi were below 800 cycles. Crack initiation cycle of solders containing Bi were smaller than that of Bi-free solders because the bigger stress amplitude was occurred for solders containing Bi. Larger crack initiation cycle of SnAgCu+NiGe as twice or three times as SnAgCu may indicates that Ni and Ge elements are useful for the long-life improving crack initiation cycle. But there is no crack initiation cycle ratio difference between SnAgCu+Bi and SnAgCu+BiNiGe. These results indicate that effect of Bi element as decreasing crack initiation cycle is more significant than effect of Ni and Ge elements as long-life improving crack initiation cycle.

Low-Ag Solders	Δε=0.3%			Δε=0.4%		
	N_i	N_f	$N_{2a=5mm}$	N_i	N_f	$N_{2a=5mm}$
Sn1.0Ag0.7Cu	1,910	14,200	19,870	1,950	12,000	17,450
Sn1.0Ag0.7CuNiGe	5,990	12,850	28,250	3,600	18,350	18,350
Sn1.0Ag0.7Cu2.0Bi	500	3,220	5,400	500	4,800	4,800
Sn1.0Ag0.7Cu2.0BiNiGe	800	2,040	2,040	150	3,180	3,200

Table 2: Crack initiation cycle (N_i), number of cycles to failure (N_f) and 5mm in crack length ($N_{2a=5mm}$).
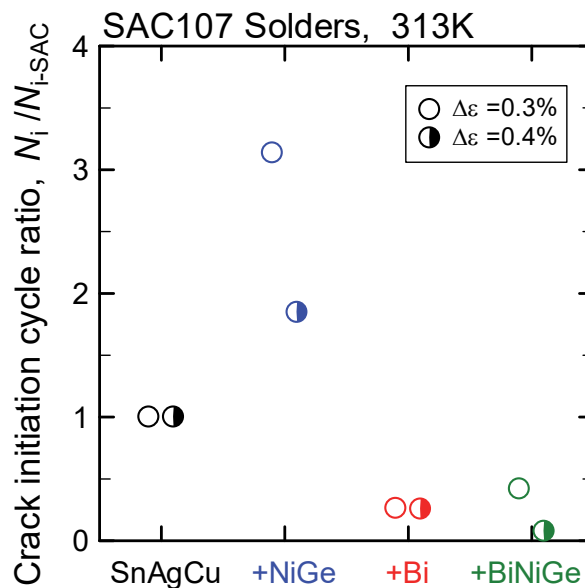

Figure 5: Effect of additive elements on crack initiation cycle.

Fig, 6 shows relationship between fatigue life ratio (N/N_f) and crack length for the four kinds of low-Ag solders at 313 K. The fatigue life ratio is the cycle number divided by the failure cycle which are listed in Tab. 2. Solid line in Fig. 6 is an average data, which is lined based on all the experimental crack length data obtained. This figure depicts that crack initiated at early stage of the fatigue cycle for all the low-Ag solders. Crack initiated at the early stage and almost all the life period was crack propagation process for the four kinds of low-Ag solders. The fatigue life ratio parameter also correlates with the crack length within a factor of 2 scatter band independent of the additive elements. These results also imply that it is important for establishing the accurate fatigue life estimation method to evaluate the crack initiation and propagation behaviour. The accurate evaluation of the crack propagation behaviour leads to the accurate fatigue life estimation.

As we mentioned above crack initiation cycles of the four kinds of low-Ag solders depend on the existence of Bi element, but effect of Ni and Ge additive elements were smaller than that of Bi element. Since it is useful to investigate the crack propagation behaviour separately from the crack initiation phenomena, crack propagation cycle (N_p) was considered in

this study as a new evaluation parameter. Crack propagation cycle was calculated as subtract the crack initiation cycle (N_i) from the total number of cycles (N).

Fig, 7 depicts crack propagation curves of the low-Ag solders, crack initiation cycle was replaced into a first cycle of the crack propagation cycle. The crack propagation of SnAgCu (colored in black) and SnAgCu+NiGe (colored in blue) seem to have a slower crack propagation rate than that of SnAgCu+Bi (colored in red) and SnAgCu+BiNiGe (colored in green). These results indicate that additive element Bi increase the crack propagation rate, but effect of additive elements Ni and Ge on the crack propagation rate are small.
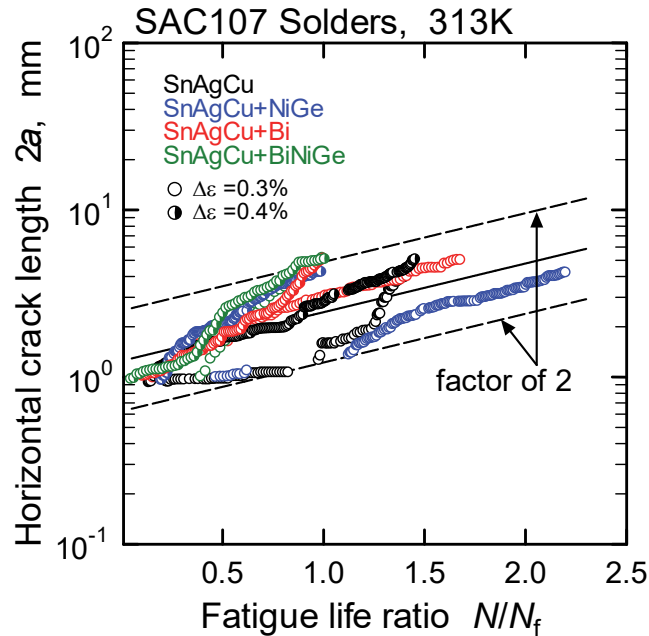

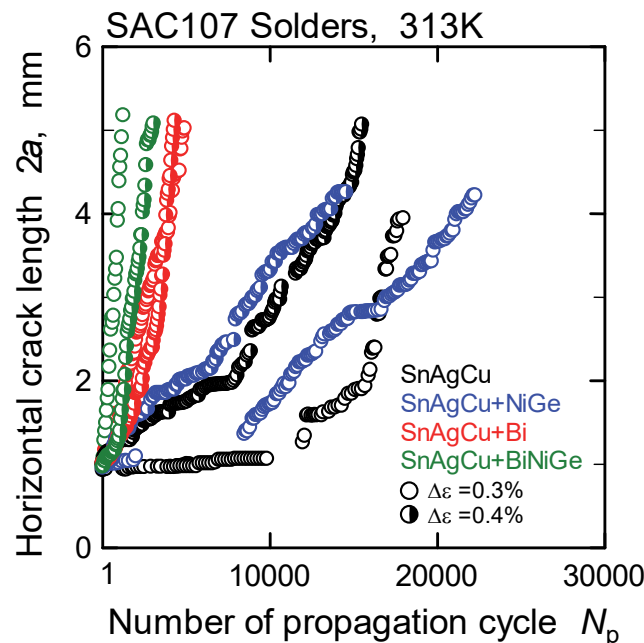Figure 6: Crack length as a function of fatigue life ratio.

Figure 7: Crack propagation curve of Sn-low-Ag-Cu solders at 313 K.

Fig, 8 shows the number of crack propagation cycles which crack length reached to 5mm for comparing the crack propagation rate. SnAgCu and SnAgCu+NiGe have almost same crack propagation cycles for both 0.3% and 0.4% strain

range. SnAgCu+Bi and SnAgCu+BiNiGe also have same crack propagation cycles at same strain range. There is no effect of additive elements Ni and Ge on the crack propagation rate, but there is Bi element effect on the crack propagation rate as shown in Fig. 8. The number of crack propagation cycle of solders containing Bi were less than half of Bi-free solders.
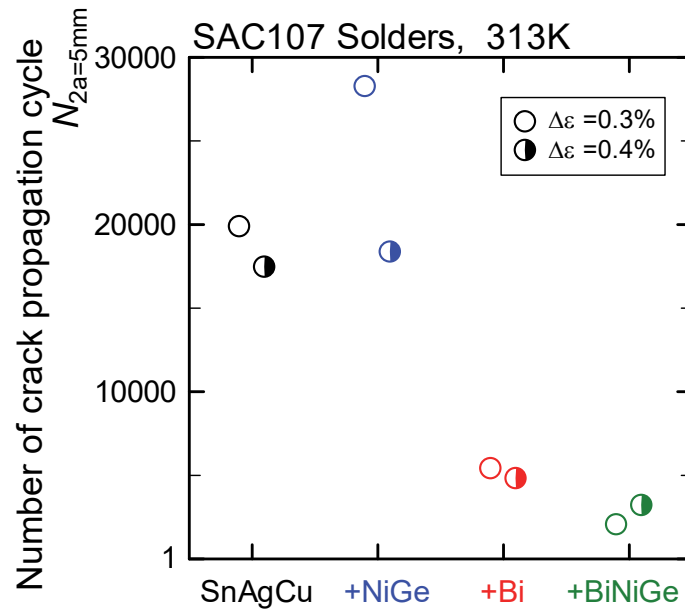

Figure 8: Effect of additive elements on crack propagation cycle.

Crack propagation rate evaluation

Because of a small proof stress and a small proportional limit for solders, almost all the total strain range is equivalent to inelastic strain range [4]. The adaptation of J-integral range parameter which is usually used for crack propagation rate evaluation of conventional steel was discussed in this study in order to evaluate the crack propagation rate of low-Ag solders. J-integral range value is calculated with Dowling method which uses an experimental data and is expressed as Eqn. (2) [9].

$$\Delta J = \frac{\left(\Delta K^*\right)^2}{E} + \frac{S}{Bb} \tag{2}$$

where, ΔK^*, E, Bb is stress intensity factor range, Young's modulus and ligament of crack-initiated specimen, respectively. S is a tensile going energy calculated as hysteresis loop area of experimental load-displacement diagram. Since a crack closer phenome was observed in the load-displacement diagram, tensile side area of a crack closer point was used for the tensile going energy calculation.

Fig, 9 shows correlation results of the crack propagation rate with J-integral range parameter. Crack propagation data of Bi-free solders are plotted in the left side of the graph, on the other hand the crack propagation data of solders containing Bi are plotted in the right side in the same graph. This data grouping trend indicates that low-Ag solders containing Bi have faster crack propagation rate and larger J-integral range value than that of the Bi-free solders.

The approximation line equation which is lined based on the experimental data at steady crack propagation stage for each low-Ag solder is expressed as follows,

for SnAgCu,
$$\frac{da}{dN} = 2.27 \times 10^{-3} \times \Delta J^{0.85} \tag{3}$$

for SnAgCu+NiGe,
$$\frac{da}{dN} = 8.72 \times 10^{-4} \times \Delta J^{0.51} \tag{4}$$

for SnAgCu+Bi,
$$\frac{da}{dN} = 1.75 \times 10^{-3} \times \Delta J^{0.73} \qquad (5)$$

for SnAgCu+BiNiGe,
$$\frac{da}{dN} = 3.29 \times 10^{-3} \times \Delta J^{0.72} \qquad (6)$$

Slope of the approximation line equations are almost same although there are data grouping due to Bi containing. This result indicates that J-integral range parameter evaluates the crack propagation rate of low-Ag solders independent of a small quantity of additive elements.

Solid line colored in orange in Fig. 9 is lined based on all the low-Ag solders experimental data. Approximation line correlates almost all the experimental data within a factor of 2 scatter band. Crack propagation rate of the steady crack propagation stage is evaluated in the narrow band with J-integral range parameter and is expressed as following equation,

$$\frac{da}{dN} = 1.09 \times 10^{-3} \times \Delta J^{0.82} \qquad (7)$$
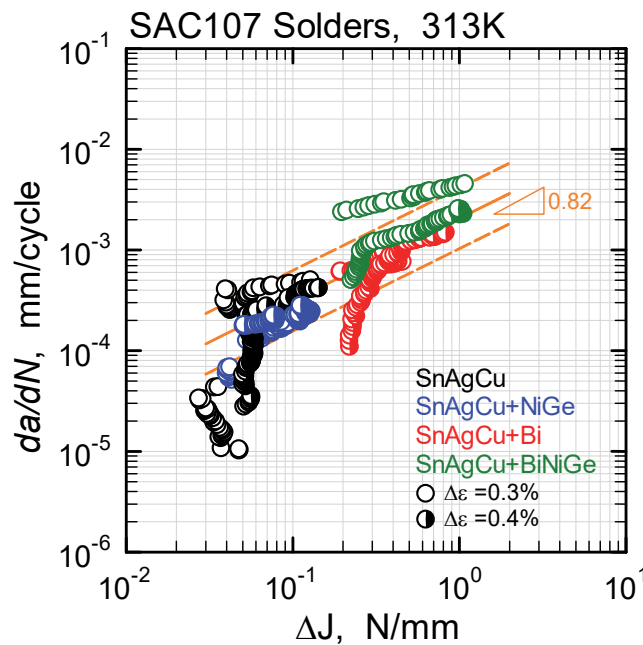

Figure 9: Relationship between crack propagation rate and ΔJ.

CONCLUSIONS

Effect of additive elements on the crack initiation and propagation behaviour of Sn-low-Ag-Cu solders were discussed in this study.

(1) Crack initiation cycle of solders containing Bi were earlier than that of Bi-free solders. Bi element hastened the crack initiation from a stress concentration part.

(2) Crack propagation rate of solders containing Bi were faster than that of Bi-free solders. Bi element also hastened the crack propagation rate during cycle fatigue process.

(3) Fatigue life ratio parameter correlates with the crack length within a factor of 2 scatter independent of the additive elements.

(4) J-integral range parameter evaluates the crack propagation rate with grouping the solders containing Bi and Bi-free solders. Slope of the approximation line equation in the J-integral range evaluation are almost same independent of the additive elements.

REFERENCES

[1] Zhu, Y., Li, X., Gao, R. and Wang, C. (2014). Low-cycle fatigue failure behavior and life evaluation of lead-free solder joint under high temperature, Microelectronics Reliability 54(12), pp. 2922–2928.

[2] Kawano, K., Naka, Y., Tanie, H., Kimoto, R. and Yamamoto, K. (2012). Fatigue Life Evaluation of Sn3Ag0.5Cu Solder Joints after High Temperature Holding, Transactions of the Japan Society of Mechanical Engineers, Series A, 78(793), pp. 1314–1324.

[3] Yamamoto, T., Itoh, T., Sakane, M. and Tsukada, Y. (2012). Creep-fatigue life of Sn-8Zn-3Bi solder under multiaxial loading, International Journal of Fatigue, 43, pp. 235–241.

[4] Hiyoshi, N., Katoh, A., Sakane, M. and Tsukada, Y. (2009). Low Cycle Fatigue Lives of Sn-37Pb and Sn-3.5Ag Solders at Low Temperatures, Journal of the Society of Materials Science, 58(2), pp. 155–161.

[5] Hiyoshi, N., Itoh, T. and Sakane, M. (2009). Development of Thermal Mechanical Fatigue Testing Machine for Solders, Journal of the Society of Materials Science, 58(2), pp. 162–167.

[6] The Society of Materials Science, Japan, Factual database on tensile, creep, low cycle fatigue and creep-fatigue of lead and lead-free solders, The Society of Materials Science, Japan (2013).

[7] Pilkey, W. D., Pilkey, D. F. (2007). Peterson's Stress Concentration Factors.

[8] The Society of Materials Science, Japan, Standard Low Cycle Fatigue Testing for Solders, The Society of Materials Science, Japan (2000).

[9] Dowling N. E. (1976). ASTM STP 601, American Society for Testing and Materials, pp. 19–32.